A NUMERICAL ASYMPTOTIC FORMULATION FOR THE POST-BUCKLING ANALYSIS OF STRUCTURES IN CASE OF COUPLED INSTABILITY

GIOVANNI GARCEA, ANTONIO BILOTTA, ANTONIO MADEO,
GIUSEPPE ZAGARI, RAFFAELE CASCIARO

Abstract. The analysis of slender structures, characterized by complex buckling and postbuckling phenomena and by a strong imperfection sensitivity, is heavily penalized by the lack of adequate computational tools. Standard incremental iterative approaches are computationally expensive and unaffordable, while FEM implementation of the Koiter method is a convenient alternative. The analysis is very fast, its computational burden is of the same order as a linearized buckling load evaluation and the simulation of different imperfections costs only a fraction of that needed to characterize the perfect structure. The main objective of the present work is to show that finite element implementations of the Koiter method can be both accurate and reliable and to highlight the aspects that require further investigation.

Key words: Koiter asymptotic analysis, coupled instability, FE method.

1. INTRODUCTION

A global evaluation of the structural collapse safety of slender elastic structures should consider all possible loadings, including the deviations due to load imperfections and geometrical defects. Standard path-following approaches, aimed at recovering the equilibrium path for a single loading case and assigned imperfections, are not suitable for this purpose. In fact in order to perform a reliable structural safety assessment the nonlinear analysis should be performed with respect to all possible imperfection shapes. The consequent computational burden can be very high particularly if no reliable information about the worst imperfection shapes is available.

The asymptotic approach, derived as a finite element implementation [1–3, 5, 10, 14, 23, 24, 32–39] of the Koiter nonlinear theory of elastic stability [28], can be a convenient alternative as it provides an effective and reliable strategy for predicting the initial post-critical behavior in both cases of limit or bifurcation points [31, 30, 6]. The implementation of the asymptotic approach as a computational tool is quite easy and its total computational burden remains of the order as that

University of Calabria, Arcavacata di Rende, CS, Italy

required by a standard linearized stability analysis. It provides the initial post-buckling behavior of the structure, including modal interactions and jumping-after-bifurcation phenomena. Moreover, once the analysis has been performed, the presence of small loading imperfections or geometrical defects can be taken into account in a post-processing phase with a negligible computational extra-cost, so allowing an inexpensive imperfection sensitivity analysis [30, 7]. It is also possible to extract information about the worst imperfection shapes [34, 8], and it can be used to improve the imperfection sensitivity analysis or for driving more detailed investigations through specialized path following analyses (see [6, 8] and references therein). From this point of view the method could be an effective tool for the evaluation of the buckling curves used in European codes [11, 13, 12]. The asymptotic analysis can provide a very accurate recovery of the equilibrium path, as it is confirmed by numerical testing and theoretical investigations [4] but requires great care in both the mechanical modeling [17, 18] and its finite element implementation. As it will be shown in the paper accuracy cannot be obtained by an inappropriate finite element interpolation due to the occurrence of interpolation locking phenomena in the evaluation of the energy variation terms used to reconstruct the post-critical behavior [31, 6]; by an inappropriate format used in the control variables that can produce extrapolation locking phenomena [20, 15]) or by the use of non-objective structural models [17, 18].

The paper is organized as follows: section 2 presents the asymptotic method, section 3 discusses all the aspects regarding the FEM implementation and the accuracy, section 4 gives some numerical results showing the potentialities of the method and finally section 5 summarizes the discussion and suggests possible extensions.

2. THE ASYMPTOTIC METHOD

In this section an asymptotic algorithm capable of treating single or multiple, also not coincident, bifurcations and of considering the effects of a nonlinear pre-critical behavior is presented. Further details can be found in [31–38].

2.1. A LYAPUNOV-SCHMIDT-KOITER ASYMPTOTIC METHOD

A brief overview of the FEM implementation of Koiter's asymptotic approach is presented here, for the convenience of the reader and to summarize the main notation and equations involved. Further details can be found in [18–31].

We consider a slender hyperelastic structure subjected to conservative loads $\lambda\hat{p}$ increasing with an amplifier factor. The equilibrium is expressed by the virtual work equation:

$$\Phi'[u]\delta u - \lambda \hat{p}\delta u = 0, \qquad \forall \delta u \in \mathcal{J}, \tag{1}$$

where $u \in \mathcal{U}$ is the field of configuration variables, $\Phi[u]$ denotes the strain energy, $\mathcal{J}$ is the tangent space of $\mathcal{U}$ at u and a prime is used for expressing the Fréchet derivative with respect to u. We assume that $\mathcal{U}$ will be a linear manifold so that its tangent space $\mathcal{J}$ will be independent from u. Eq. (1) defines a curve in the (u, λ) space, the *equilibrium path* of the structure, that can be composed of several branches. We are usually interested in the branch starting from an initial known equilibrium point u_0, λ_0 and without any loss of generality we can assume $u_0 = 0$, $\lambda_0 = 0$. It is worth mentioning that a mixed format is generally convenient to avoid the so called nonlinear locking phenomena [20, 15, 22], so configuration u usually collects both displacement and stress fields.

The asymptotic method is based on an expansion of the potential energy, in terms of load factor λ and buckling mode amplitudes ξ_i, which is characterized by fourth-order accuracy. It provides an approximation of the equilibrium path by performing the following steps:

1. The fundamental path is obtained as a linear extrapolation, from a known equilibrium configuration:

$$u^f[\lambda] = \lambda \hat{u}, \tag{2}$$

where $\hat{u}$ is the tangent $\{0; 0\}$, obtained as a solution of the linear equation

$$\Phi_0'' \hat{u}\delta u = \hat{p}\delta u, \qquad \forall \delta u \in \mathcal{J} \tag{3}$$

and an index denotes the point along u^f for which the quantities are evaluated, that is $\Phi_0'' \equiv \Phi''\left[u^f[\lambda_0]\right]$.

2. A cluster of buckling loads $\{\lambda_0 \ldots \lambda_m\}$ and associated buckling modes ($\dot{v} \ldots \dot{v}_m$) are defined along $u^f[\lambda]$ by the critical condition

$$\Phi''\left[u^f[\lambda_i]\right]\dot{v}_i\delta u = 0, \qquad \forall \delta u \in \mathcal{J}, \tag{4}$$

Buckling loads are considered to be sufficiently close to each other to allow the following linearization

$$\Phi_b''' \dot{v}_i \delta u + (\lambda_i - \lambda_b)\Phi_b''' \hat{u}\dot{v}_i\delta u = 0, \qquad \forall \delta u \in \mathcal{J}, \tag{5}$$

λ_b being an appropriate reference value of λ (e.g. the first of λ_i or their mean value). Normalizing, we obtain $\Phi_b''' \hat{u}\dot{v}_i\dot{v}_j = \delta_{ij}$, where δ_{ij} is Kroneker's symbol.

3. The tangent space $\mathcal{J}$ is decomposed into the tangent $\mathcal{V} \equiv \{\dot{v} = \Sigma_i \dot{v}_i\}$ and orthogonal $\mathcal{W} \equiv \{w : \Phi_b''' \hat{u} \dot{v}_i w = 0\}$ subspaces so that $\mathcal{J} = \mathcal{V} \oplus \mathcal{W}$. Making and $\xi_0 = \lambda$ and $\dot{v}_0 = \hat{u}$, the asymptotic approximation for the required path is defined by the expansion

$$u[\lambda, \xi_k] \equiv \sum_{i=0}^{m} \xi \dot{v}_i + \frac{1}{2} \sum_{i=0}^{m} \xi_i \xi_j w_{ij}, \tag{6}$$

where w_{ij} are quadratic corrections introduced to satisfy the projection of eq. (1) onto $\mathcal{W}$ and obtained by the linear *orthogonal equations*

$$\Phi_b'' w_{ij} \delta w = -\Phi_b''' \dot{v}_i \dot{v}_j \delta w, w_{ij} \qquad \delta w \in \mathcal{W}, \tag{7}$$

where, because of the orthogonality condition, $w_{0i} = 0$.

4. The following energy terms are computed for $i, j, k = 1 \ldots m$:

$$\mu_k[\lambda] = \frac{1}{2} \lambda^2 \Phi_b''' \hat{u}^2 \dot{v}_k + \frac{1}{6} \lambda^2 (\lambda - 3\lambda_b) \Phi_b''' \hat{u}^3 \dot{v}_k$$

$$A_{ijk} = \Phi_b''' \dot{v}_i \dot{v}_j \dot{v}_k$$

$$B_{ijhk} = \Phi_b'''' \dot{v}_i \dot{v}_j \dot{v}_h \dot{v}_k - \Phi_b'' (w_{ij} w_{hk} + w_{ih} w_{jk} + w_{ik} w_{jh}) \tag{8}$$

$$B_{00jk} = \Phi_b'''' \hat{u}^2 \dot{v}_i \dot{v}_k - \Phi_b'' w_{00} w_{ik}$$

$$B_{0ijk} = \Phi_b'''' \hat{u} \dot{v}_i \dot{v}_j \dot{v}_k$$

$$C_{ik} = \Phi_b'' w_{00} w_{ik},$$

where the *implicit imperfection factors* μ_κ are defined by the 4th order expansion of the unbalanced work on the fundamental (i.e. $\mu_k[\lambda] = (\lambda \hat{p} - \Phi'[\lambda \hat{u}]) \dot{v}_k$).

5. The equilibrium path is obtained by satisfying the projection of the equilibrium equation (1) onto $\mathcal{V}$. According to eqs. (7) and (8), we have

$$\begin{aligned} &(\lambda_k - \lambda) \xi_k - \lambda_b \left(\lambda - \frac{\lambda_b}{2} \right) \sum_{i=1}^{m} \xi_i C_{ik} + \frac{1}{2} \sum_{i,j=1}^{m} \xi_i \xi_j A_{ijk} + \\ &+ \frac{1}{2} (\lambda - \lambda_b)^2 \sum_{i=1}^{m} \xi_i B_{00ik} + \frac{1}{2} (\lambda - \lambda_b) \sum_{i,j=1}^{m} \xi_i \xi_j B_{0ijk} + \\ &+ \frac{1}{6} \sum_{i,j,k=1}^{m} \xi_i \xi_j \xi_h B_{ijhk} + \mu_k[\lambda] = 0, \qquad k = 1 \ldots m. \end{aligned} \tag{9}$$

Equation (9) corresponds to a highly nonlinear system in the $m + 1$ unknowns $\lambda - \xi_i$ and can be solved using a standard path-following strategy. It provides the initial post-buckling behavior of the structure, including *modal interactions* and *jumping-after-bifurcation* phenomena.

2.2. IMPERFECTION SENSITIVITY ANALYSIS

When analyzing a structure, it is difficult to characterize its geometry and loads exactly, for the presence of a random distribution of small *external imperfections*. This circumstance, also if the general behavior of the structure is preserved, changes some aspects of its response and often causes a reduction in the carrying capacity.

In the proposed asymptotic algorithm the presence of small additional imperfections expressed by a load $\varepsilon_q \tilde{q}[\lambda]$ and/or an initial displacement $\varepsilon_q \tilde{u}$ affect Eq. (9) only with the imperfection term $\mu_k[\lambda]$ that becomes [31, 30, 6]

$$\mu_k = \frac{1}{2}\lambda^2 \Phi_c''' \hat{u}^2 \nu_k + \frac{1}{6}\lambda^2 (\lambda - 3\lambda_c) \Phi_c'''' \hat{u}^3 \nu_k + \mu_k^1[\lambda] + \mu_k^g[\lambda], \tag{10}$$

with

$$\mu_k^1[\lambda] = -\varepsilon \tilde{q}[\lambda] \nu_k, \qquad \mu_k^g[\lambda] = \lambda \Phi_c''' \hat{u} \tilde{u} \nu_k. \tag{11}$$

The aim of the *imperfection sensitivity analysis* is to link the presence of geometrical and load imperfections to the reduction in the limit load. For structures presenting coupled buckling even a small imperfection in loading or geometry can mean a marked reduction in collapse load with respect to the bifurcation load [11, 13, 12]. So an effective safety analysis should include an investigation of all possible imperfection shapes and sizes to recover, albeit in a statistical sense, the worst case.

The asymptotic approach provides a powerful tool for performing this extensive investigation. In fact, the analysis for a different imperfection only needs to update the imperfection factors $\mu_k^g[\lambda]$ and $\mu_k^l[\lambda]$ through Eq. (11) and to solve once more the nonlinear system (9). Even if this system, collecting all the nonlinear parts of the original problem, proves to be highly nonlinear and some care has to be taken in treating the occurrence of multiple singularities, its solution through a path-following process is relatively simple because of the small number of unknowns involved.

However, exhaustive results can only be obtained in a statistical context linking the distribution probability of the imperfection to that of the load. An effective imperfection sensitivity analysis can be performed by a Monte-Carlo

statistical technique, where both the magnitude and the form of the imperfections are treated as random variables. The analysis is then performed by taking the additional imperfection factors in the form

$$\mu_k^l[\lambda] + \mu_k^g[\lambda] = \lambda\left(\tilde{q}[\lambda] - \Phi_c''' \hat{u}\tilde{u}\dot{v}_k\right) = \lambda\overline{\mu}_k, \tag{12}$$

and producing a random sequence of imperfection vectors $\overline{\boldsymbol{\mu}} = \{\overline{\mu}_1, \overline{\mu}_2 ... \overline{\mu}_m, \}$, modeling possible small deviations in the loads and in the geometry of the structure, and repeating a path-following solution of (9) for each of these. By a statistical treatment of the obtained results we obtain the probability distribution function for the limit load multiplier and all the other useful statistical information. This solution process, can be considered as a standard approach for imperfection sensitivity analysis [8]. The number of repetitions needed to obtain statistically reliable results increases (quite) exponentially with the number of the buckling modes and for large *m* can become very expensive. The imperfection sensitivity analysis can however be performed in a simple and efficient way when a criterion for defining the (few) 'significant' imperfection forms is available [34].

2.3. ATTRACTIVE PATH THEORY

A large number of different imperfections (up to several thousands) has to be considered to obtain statistically significant results, so, while the analysis for a single imperfection can be considered an easy task, the entire solution process performed proves to be computationally expensive, especially when a large number of coupled buckling modes have to be considered. We can, however, noticeably reduce the computational effort by exploiting information given by the knowledge of the complete set of attractive radial paths

$$\xi_i = t\xi_i^*, \qquad i = 1 ... m, t \in \mathbb{R} \tag{13}$$

which are local minimizers for the cubic form

$$\dot{\lambda}_b = \frac{1}{2}\sum_{i,j,h=1}^{m} A_{ijh}\xi_i^*\xi_i^*\xi_h^* = \underbrace{min}_{(\xi_k^*)}, \qquad \sum_{i=1}^{m}\xi_i^*\xi_i^* = 1 \tag{14}$$

or for the quartic form

$$\ddot{\lambda}_b = \frac{1}{3}\sum_{i,j=1}^{m} B_{ijhk}\xi_i^*\xi_i^*\xi_h^*\xi_k^* = \underbrace{min}_{\xi_k^*}, \qquad \sum_{i=1}^{m}\xi_i^*\xi_i^* = 1 \tag{15}$$

on the unit hypersphere.

Attractive paths theory [8, 25, 26, 29, 34] can actually provide a helpful tool for driving the analysis and reducing its total cost. In fact, it suggests that each imperfect path obtained from the solution of (9) will be attracted by one of the

minimizing radial directions ξ^* (see Fig. 7 in the numerical results section). Then, an evaluation for the limit load associated to the single imperfection vector $\bar{\boldsymbol{\mu}}$ can be obtained by performing a series of different monomodal analyses, one for each minimum radial path (13), and then taking the smallest value obtained for the limit load within all directions. The single monomodal analysis is quite quick, so a large number of different imperfections can be investigated rapidly with results, in terms of limit load distribution, equivalent to that provided by a full analysis [8].

Furthermore, it is worth mentioning that, once the worst imperfection shapes have already been obtained from an imperfection sensitivity analysis, a detailed investigation can be performed through a specialized path-following analysis, taking into account these imperfections [27, 22].

3. ACCURACY AND EFFICIENCY IN FINITE ELEMENT IMPLEMENTATION OF THE ASYMPTOTIC ANALYSIS

In the following we present a numerical formulation of the method suitable for implementation using finite elements and discuss some aspects that are crucial to achieve accuracy and efficiency.

3.1. FE IMPLEMENTATION OF ASYMPTOTIC METHOD

Applying a FE interpolation $u = \mathcal{L}\boldsymbol{u}$, $\mathcal{L}$ being the interpolation operator and $\boldsymbol{u}$ the vector collecting the discrete displacement and stress parameters, the asymptotic analysis requires the following steps:

i. The *fundamental path* is obtained introducing the linear extrapolation

$$\boldsymbol{u}^f[\lambda] = \boldsymbol{u}_0 + \lambda\hat{\boldsymbol{u}}, \tag{15}$$

where $\hat{\boldsymbol{u}}$ is the initial path tangent, solution of the linear vectorial equation

$$\mathbf{K}_0\hat{\boldsymbol{u}} = \hat{\boldsymbol{p}}, \tag{17}$$

$\mathbf{K}_0$ being the stiffness matrix evaluated for $\boldsymbol{u} = \boldsymbol{u}_0$ and $\hat{\boldsymbol{p}}$ the unitary load vector, defined by the energy equivalencies

$$\delta\boldsymbol{u}^{\mathrm{T}}\mathbf{K}[u]\dot{\boldsymbol{u}} = \Phi''[u]\dot{u}\delta u, \qquad \delta\boldsymbol{u}^{\mathrm{T}}\hat{\boldsymbol{p}} = \hat{p}\delta u.$$

The solution of linear system (17) requires a standard factorization of $\mathbf{K}_0$.

ii. A cluster of *buckling loads* $\lambda_i, i = 1...m$, and associated *buckling modes* $\dot{\boldsymbol{v}}_i$ are obtained along $\boldsymbol{u}^f[\lambda]$ exploiting the critical condition

$$\mathbf{K}[\lambda_i]\dot{\boldsymbol{v}}_i = 0, \qquad \mathbf{K}[\lambda] = \mathbf{K}[\boldsymbol{u}_0 + \lambda\hat{\boldsymbol{u}}]. \tag{18}$$

This corresponds to a nonlinear eigenvalue problem which can be linearized and solved using standard algorithms and exploiting matrix $\mathbf{K}_0^{-1}$, already available from the previous step, to perform the iterations [7].

iii. Letting λ_c be an appropriate reference value for the cluster, e.g. the smallest of λ_i or their mean value, the asymptotic approximation for the required path is defined by the expansion

$$\boldsymbol{u}\left[\lambda,\xi_k\right] = \boldsymbol{u}_b + \sum\nolimits_{i=0}^{m} \xi_i \dot{\boldsymbol{v}}_i + \frac{1}{2}\sum\nolimits_{i,j=0}^{m} \xi_i \xi_j \boldsymbol{w}_{ij}, \tag{19}$$

where the quadratic corrections $w_{ij} \in \mathcal{W}$ are obtained by the linear orthogonal equations

$$\delta\boldsymbol{w}^{\mathrm{T}}\left(\mathbf{K}_c \boldsymbol{w}_{ij} + \boldsymbol{p}_{ij}\right) = 0, \qquad \forall \boldsymbol{w} \in \mathcal{W} \tag{20}$$

with $\mathbf{K}_c = \mathbf{K}\,[u^f \lambda_c]$ and vectors $\boldsymbol{p}_{ij}$ defined as a function of modes $\dot{\boldsymbol{v}}_i$ and $i = 0\ldots m$ obtained by an element-by-element assembling process using the energy equivalence

$$\delta\boldsymbol{w}^{\mathrm{T}}\boldsymbol{p}_{i,j} = \Phi_c''' \,\delta w \dot{v}_i \dot{v}_j. \tag{21}$$

The solution of linear system (20) can be conveniently obtained, as described in [7, 6], through a Modified Newton-like iteration scheme exploiting $\mathbf{K}_0^{-1}$ as iteration matrix.

iv. The *energy terms* in (9) being scalar quantities are evaluated as a sum, at the element level, of the integrals of known functions.

v. The equilibrium path is obtained by solving the algebraic nonlinear system of m equations in the $m + 1$ variables $\xi_0, \xi_1 \ldots \xi_m$ defined in Eq. (9) using a path-following algorithm. Because of the small dimensions of the system, this can be obtained very quickly using standard or even specialized variants of the arc-length scheme.

The actual implementation of the asymptotic approach as a computational tool is therefore quite easy in practice and its total computational burden, which is mainly involved in the factorization of matrix $\mathbf{K}_0$, remains of the order of that required by a standard linearized stability analysis. It provides the initial post-buckling behavior of the structure, including *modal interactions* and *jumping-after-bifurcation* phenomena. Moreover, once the preprocessing phase of the analysis has been performed (steps i to iv), the presence of small loading imperfections or geometrical defects can be taken into account in the postprocessing phase (step v), by adding some, easily computed, additional imperfection terms in the expression of $\mu_k[\lambda]$, with a negligible computational extra-cost, so allowing an inexpensive imperfection sensitivity analysis [30, 15].

Imperfection sensitivity analysis can be simplified by evaluating all the minimum directions of the cubic (14) and quartic forms (14) to obtain the worst

imperfection directions as discussed in subsection 2.2.1. Today this is not a completely solved problem and it can also be expensive. Nevertheless, relative minimum solutions can be (quite easily) obtained by using the iterative scheme suggested in [34]. Furthermore for the case of symmetric buckling, problem (15) can be transformed into a non-convex Quadratic Problem subject to linear constraints and solved using the strategy presented in [8].

3.2. ON THE ACCURACY OF THE ASYMPTOTIC FORMULATION

The method, as will be shown in the numerical results section, is potentially capable of furnishing accurate results if a series of modelling and implementation aspects are carefully tuned. In the following we quickly present some of the sources of inaccuracy referring readers to the references for a deeper discussion.

3.2.1. Interpolation locking

In the asymptotic algorithm a locking phenomenon related to the discretization process can arise from the evaluation of the fourth-order terms

$$B_{ijhk} = \Phi_c''' \dot{\mathrm{v}}_i \dot{\mathrm{v}}_j \dot{\mathrm{v}}_h \dot{\mathrm{v}}_k - \Phi_c'' (\ddot{w}_{ij} \ddot{w}_{hk} + \ddot{w}_{ih} \ddot{w}_{jk} + \ddot{w}_{ik} \ddot{w}_{jh}),$$

that define the initial curvature of the post-buckling path. The coefficients B_{ijhk} are obtained as the difference between two quantities derived from the fourth and second variations. In compatible formulations the single term of this difference is, usually, very large while the difference is small. The discretization error on the single term could in this case be greater than the small results in their difference. Obviously, the numerical response given by the asymptotic algorithm in this case is completely unreliable.

The size of the error produced by this locking pathology depends on the finite element interpolation functions and decreases for an appropriate balancing of the polynomial functions used to describe each displacement component. The phenomenon is particular evident for beam and plate structures where the buckling modes $\dot{\mathrm{v}}_i$ usually contain only flexural displacement components while $\ddot{w}_{ij}$ only in plane or axial ones. The locking is sanitized when a mixed finite element is used [31, 6].

Figure 1, which refers to a planar Euler rod case reports numerical results for the post-buckling factor $\ddot{\lambda}_b = B_{1111}$ obtained for different values of the ratio EAL^2/EJ between the axial and the flexural stiffness, by using an element called HC [31] that uses the same quadratic spline functions for both the transversal and the axial components and standard beam elements (linear and cubic interpolation for the axial and transversal displacements, respectively).

Note that, for $EAL^2/EJ = 1.2 \cdot 10^5$, 20 HC elements are sufficient to contain the error in $\ddot{\lambda}_b$ at under 1% while standard discretizations do not yield reliable results even using a large number of elements. A mixed finite element completely sanitizes this pathological phenomenon.

3.2.2. Extrapolation locking

Mixed or compatible formats, while completely equivalent in principle, behave very differently when implemented in asymptotic but also in path-following solution strategies. This is an important, even if frequently misunderstood, point in practical computations which has been widely discussed in [21, 20, 15, 16, 6]. By referring readers to these papers for more details, we only recall here that both numerical strategies need function Φ and its Hessian $\mathbf{K}[\boldsymbol{u}]$ to be appropriately smooth in its controlling variables. In path-following analysis, this ensures a fast convergence of the Newton iterative process; in asymptotic analysis, it implies that the higher-order energy term neglected in the Taylor expansion be really irrelevant, allowing an accurate recovery of the equilibrium path. We know that the smoothness of a nonlinear function strictly depends on the choice of the set of its control variables, that is on the format of its description, and can change noticeably when referring to another, even corresponding, set. As a consequence, the mixed and compatible format, even if referring to the same problem, can be characterized by a different smoothness and so they behave differently in practice, when used within a numerical solution process. Actually, the compatible format is particularly sensitive to what we call *extrapolation locking* in [20, 15] which can produce a loss in convergence when used in path-following analyses, or unacceptable errors in the path recovery in the asymptotic case. These inconveniences are easily avoided by changing to a mixed format.

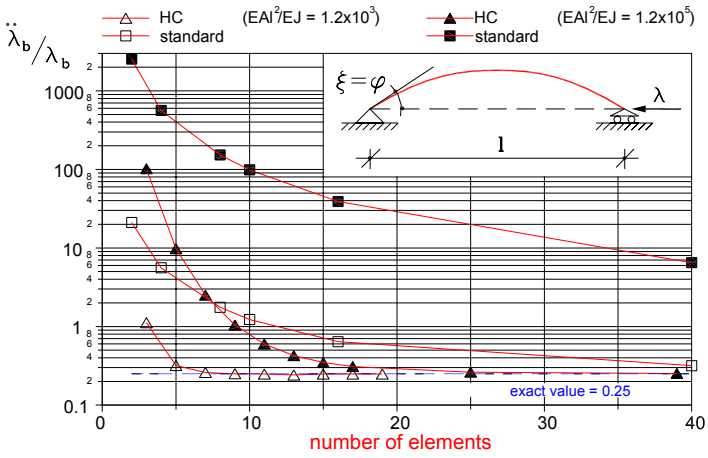

Fig. 1 – Locking in the Euler case [30].

3.2.3. Objective structural model

The asymptotic analysis makes great use of information attained from a fourth-order expansion of the strain energy and then requires a fourth-order accuracy be guaranteed in the structural modeling. Small inaccuracies, deriving from geometrical incoherencies in the higher-order terms of the expansion of the kinematical laws or in its finite element representation, significantly affect the accuracy of the solution and can make it unreliable. Structural models not affected by rigid body motions or by changes in observer are then required. This aspect is more important with respect to the path-following case where only the first variation needs to be correctly evaluated. With this aim the *Implicit Corotational Method (ICM)* [17, 18] has been proposed as a tool to obtain geometrically exact nonlinear models for structural elements, such as beams or shells, undergoing finite rotations and small strains starting from the solutions for the 3D Cauchy continuum used in the corresponding linear modeling. The main idea is to associate a corotational frame to each point of the 3D continuum so allowing the motion in the neighbor of the point to be split in a pure stretch followed by a pure rotation, according to the decomposition theorem. It is possible to show how, using the small strain hypothesis and rotation algebra, the linear stress and linear strain fields, when viewed in this corotational frame, can provide accurate approximations for the Biot nonlinear stress and strain fields. Once the corotational rotation is appropriately defined, the local statics and kinematics of the model are recovered from the linear solution as a function of the stress/displacement resultants. Stress and strain fields are then introduced within a mixed variational principle in order to obtain the constitutive laws directly in terms of stress/strain resultants. This completes the ICM definition of the nonlinear model.

The nonlinear model so obtained retains all the details of the 3D linear solution, including torsion/shear warping, while its objectivity is ensured implicitly. Furthermore, the use of the mixed formulation and the greater accuracy with which the ICM recovers the stress field, allows an accurate description of the constitutive laws in terms of resultants. ICM does not require any ad-hoc assumption about the structural model at hand, nor depends on any particular parametrization of the rotation tensor, but actually behaves as a black-box tool able to translate known linear models into the corresponding nonlinear ones. Moreover, the direct use of a mixed (stress/strain) description provides an automatic and implicitly coherent methodology for generating models free of the nonlinear locking effects previously discussed, in a format directly suitable for use in FEM implementations. The method was applied in [17] to derive 3D beam and plate nonlinear models starting from the Saint Venànt rod and Kirchhoff and Mindlin-Reissner plate linear theories, respectively.

4. NUMERICAL RESULTS

Some results regarding the analysis of both 3D beams and plates are reported and compared with particular reference to accuracy as previously discussed. In the monomodal buckling tests, to compare the accuracy with known solutions, the following quantities, defining the postcritical tangent and curvature to the bifurcated path, have been introduced

$$\dot{\lambda}_b = -\frac{1}{2}\frac{A_{111}}{A_{011}}, \qquad \ddot{\lambda}_b = -\frac{B_{1111} + 3\dot{\lambda}_b^2 B_{0111} + 3\lambda_b^2 B_{0011}}{3A_{011}}.$$

The results are compared with known analytical solutions (see [6]) and with the ones obtained using the *LC* (Complete Lagrangian) and *LS* (Simplified Lagrangian) technical plate models (see [15, 22] for a discussion on these models) already implemented in the code named KASP. An independent analysis has also been made using the commercial code ABAQUS.

4.1. THE INFLUENCE OF THE STRUCTURAL MODEL

The test refers to the Euler beam shown in Fig. 2. The beam is analyzed forcing the buckling to have in-plane or out-of-plane components only. Despite its simplicity, when analyzed with an asymptotic approach, the problem is taxing with regard to the accuracy of the structural model and its FEM discretization [18]. In Fig. 2 the values of the buckling loads and post-critical curvatures are compared with the values obtained by using the Antman beam model and exact interpolation functions [6]. The ICM model recovers the analytical solution for sufficiently fine grids exactly. The *LC* and *LS* models provide a correct answer for the buckling load, but have a different post-buckling behavior in the in-plane or out-of-plane analysis: *LC* agrees perfectly with the exact solution in the in-plane case, whereas *LS* provides the wrong result $\ddot{\lambda}/\lambda_B = 2,$ which is eight times greater; conversely, *LS* behaves better in the out-of-plane case, by providing the approximation $\ddot{\lambda}/\lambda_B = 0,$ while *LC* gives a completely erroneous unstable postbuckling curvature $\ddot{\lambda}/\lambda_B = 0.75.$ The resulting paths in Fig. 3 show a good agreement with those computed by path-following analyses.

Table 1

	Out plane				**In plane**			
	N. elm.	*LC*	*LS*	*ICM*	*LC*	*LS*	*ICM*	*2D Beam*(*)
λ_b	16	9.901	9.901	9.901	9.918	9.918	9.918	
	32	9.877	9.877	9.877	9.870	9.870	9.870	9.870
	64	9.872	9.872	9.871	9.867	9.870	9.870	
$\frac{\ddot{\lambda}_b}{2\lambda_b}$	16	-0.354	0.020	0.145	0.166	1.03	1.03	
	32	-0.375	0.000	0.125	0.126	1.00	1.00	9.870
	64	-0.375	0.000	0.125	0.125	1.00	1.00	

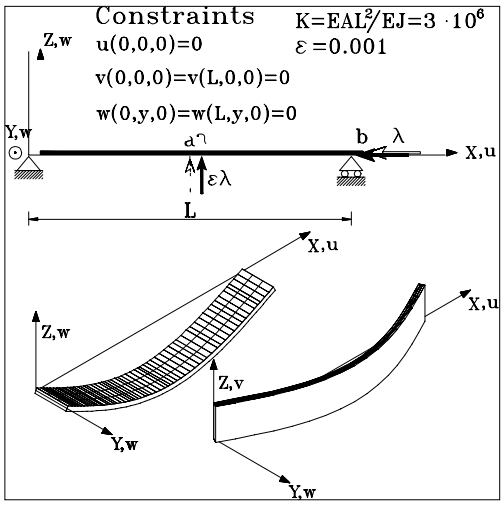

Fig. 2 – Euler beam: problem description and buckling and post-buckling parameters [31].

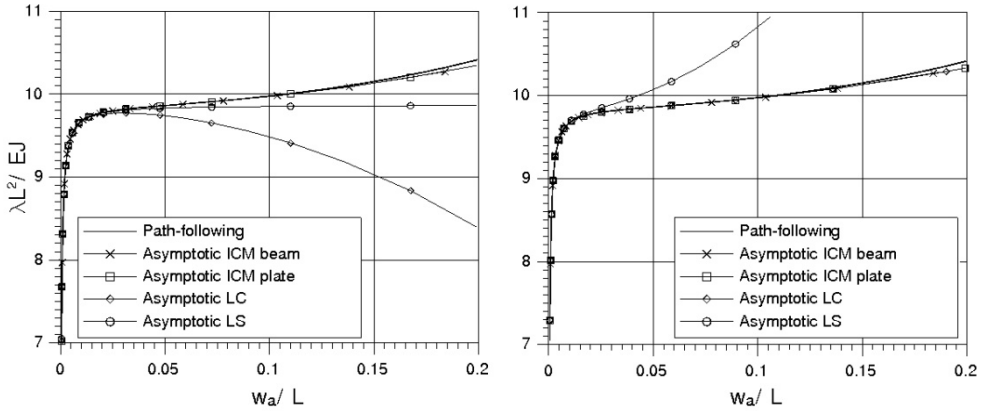

Fig. 3 – Euler beam: out-plane and in-plane equilibrium path [31].

4.2. TEST WITH NONLINEAR PRECRITICAL BEHAVIOUR

The test in Fig. 4 is relative to a structure characterized by a highly nonlinear pre-critical behavior. The first two buckling loads are equal to $\lambda_1 = 4.52$ and $\lambda_2 = 7.11,$ while the limit load is almost an half of the minimum buckling value and is evaluated exactly as can be observed by the comparison with the asymptotic and path-following (ABAQUS) curve denoted respectively CR4 and SR8. It is worth of noting that only the implicit imperfection acts on the structure.

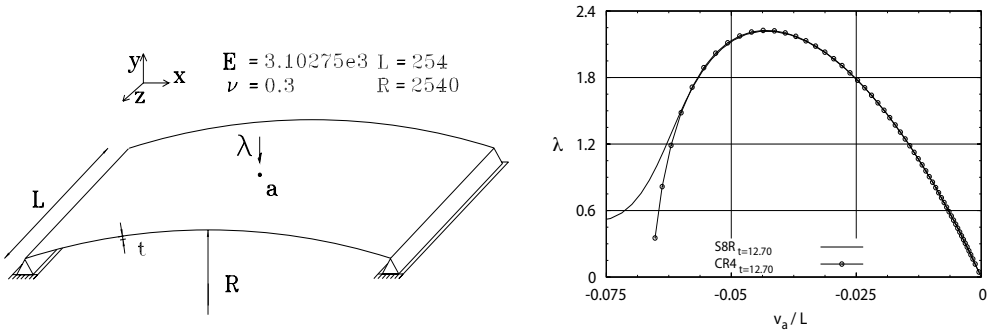

Fig. 4 – Hinged cylindrical shell [41].

4.3. MULTIMODAL BUCKLING AND ATTRACTIVE PATH

The first test is the thin-walled beam in Fig. 5 modeled as a plate assemblage.

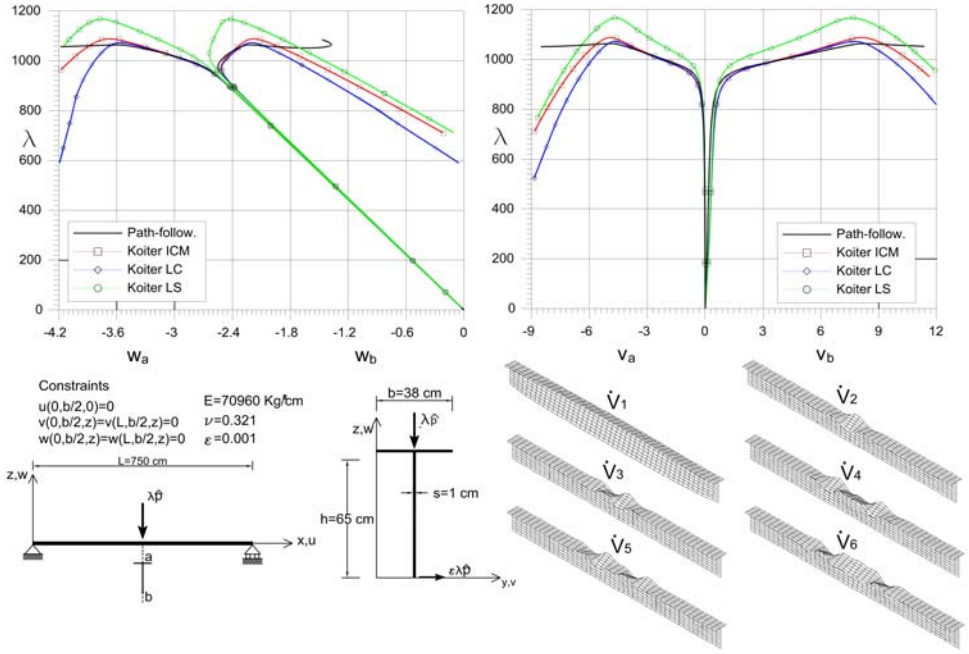

Fig. 5 – T beam: problem description, buckling modes and equilibrium paths [31, 6].

The model is that proposed in [17, 18] on the basis of the ICM and is denoted as MP in the results. The results are compared with those of an ABAQUS analysis using a path-following approach and of the technical plate models [15]. The greater accuracy of the objective structural model is evident in Fig. 5 where the equilibrium paths are depicted.

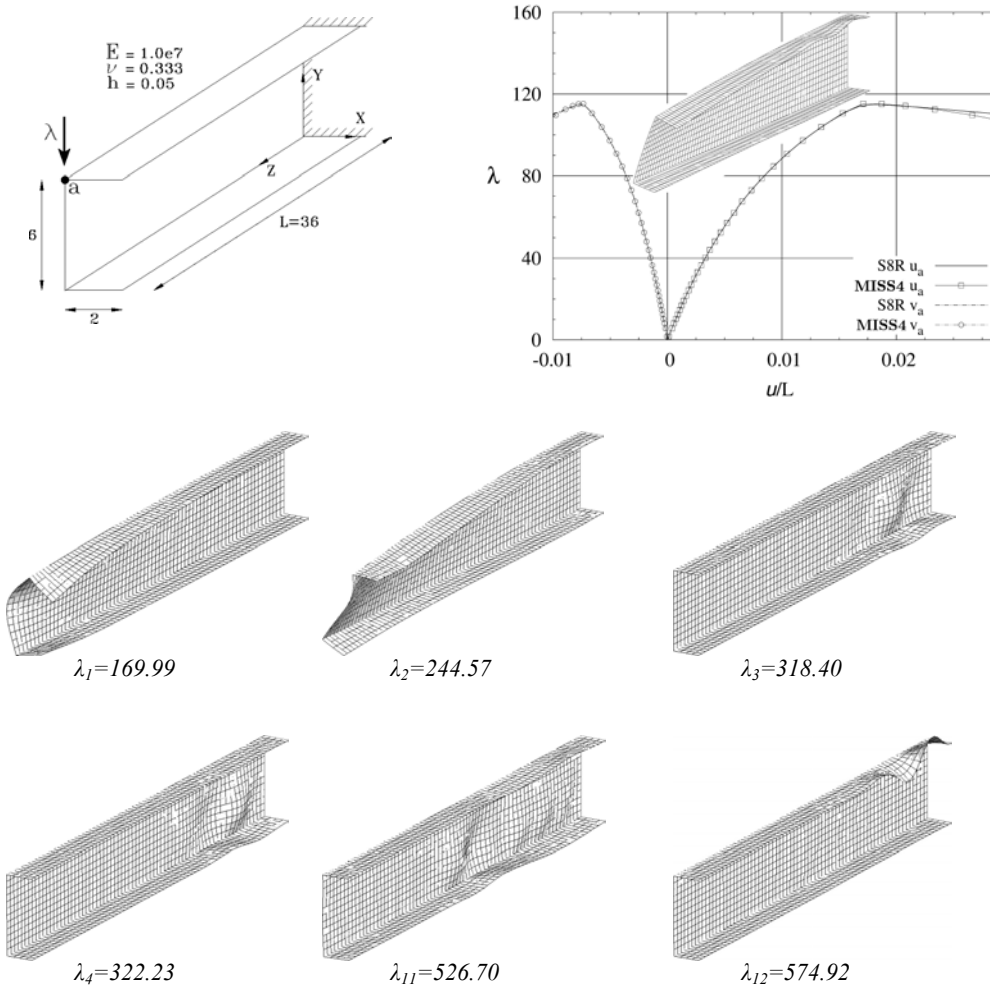

Fig. 6 – C-shaped cantilever beam [41].

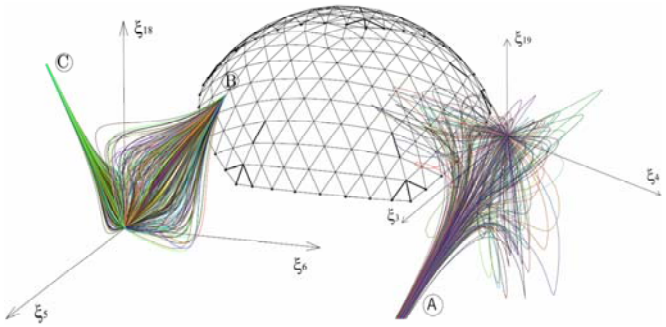

Fig. 7 – Geodetic dome: modal interaction between 20 critical modes [8].

The second case regards a C-shaped cantilever beam subjected to a single force at the free end reported in Fig. 6. In this case the strong modal interaction between non near buckling loads also produce a highly unstable behaviour as shown by the equilibrium path.

Finally the last test regards the Geodetic Dome modeled through a 3D truss as proposed in [8]. In this case many locally coincident buckling modes interact and the structure exhibits a very marked unstable behavior. In Fig. 7, in the modal space ξ_k different equilibrium paths, clearly converging along only one of the minimum directions, are reported. The test shows how it is possible to perform the sensitivity analysis in a simplified way along the predetermined quartic form minimum directions.

5. CONCLUSION

The paper presented the numerical implementation of the Koiter asymptotic approach to evaluate the buckling and postbuckling behaviour of geometrically nonlinear structures in the case of multiple coincident buckling loads and random external imperfections. Standard techniques, based on repeated path-following analyses, are useful for a thorough investigation of the structural behaviour with a single imperfection shape, but cannot be considered effective tools to predict the safety factor for geometrically nonlinear problems. The asymptotic method, instead, appears to be an attractive alternative as it allows a reliable analysis with computational costs similar to those required by a standard load buckling prediction, while subsequent analyses for different imperfections are inexpensive.

The method furnishes accurate results and also information about the worst imperfection shape if a series of modeling and implementation aspects are carefully tuned. In particular it was shown how the effects of the use of geometrically exact structural models and their coherent finite element implementation are very relevant, while a mixed formulation eliminates both interpolation and extrapolation locking phenomena.

Received on July 16, 2014

REFERENCES

1. Arbocz, J., Hol, J. M. A. M., *Koiter's stability theory in a computer-aided engineering (CAE) environment*, Int. J. Solids Struct, **26**, pp. 945–973, 1990.
2. Barbero, E. J., Godoy, L. A., Raftoyiannis I. G., *Finite elements for three-mode interaction in buckling analysis*, Int. J. Numer. Meth. Eng, **39**, pp. 469–488, 1996.
3. Boutyour, E. H., Zahrouni, H., Potier-Ferry, M., Boudi, M., *Asymptotic-numerical method for buckling analysis of shell structures with large rotations*, Journal of Computational and Applied Mathematics, **168**, *1–2*, pp. 77–85, 2004.

4. Brezzi, F., Cornalba, M., Di Carlo, A., *How to get around a simple quadratic fold*, Numer. Math, **48**, pp. 417–427, 1986.
5. Budiansky, B., *Theory of buckling and post–buckling of elastic structures*, Advances in Applied Mechanics, **14**, Academic Press, New York, 1974 .
6. Casciaro R., Computational asymptotic post-buckling analysis of slender elastic *structures*, CISM Courses and Lectures No. 470, SpringerWien, New York, 2005.
7 Casciaro, R., Garcea, G., Attanasio, G., Giordano, F., *Perturbation approach to elastic postbuckling analysis*, Comput. Struct, **66**, 585–595, 1998.
8. Casciaro R., Mancusi G., *Imperfection sensitivity due to coupled local instability: a nonconvex QP solution algorithm*, Int. J. Numer. Meth. Eng, **67**, pp. 815–840, 2006.
9. Casciaro R., Salerno G., Lanzo A. D., *Finite Element Asymptotic Analysis of Slender Elastic Structures: a Simple Approach*, Int. J. Numer. Meth. Eng, **35**, pp. 1397–1426, 1992.
10. Chen, H., Virgin, L. N., *Finite element analysis of post-buckling dynamics in plates*, *Part I: An asymptotic approach*, Int. J. Solids Struct, **43**, pp. 3983–4007, 2006.
11. Dubina, D., *The ECBL approach for interactive buckling of thin-walled steel members*, Steel and Composite Structures, **1**, *1*, pp. 7596, 2001.
12. Dubina, D., Ungureanu, V., *Instability mode interaction: From Van Der Neut model to ECBL approach*, Thin-Walled Structures, Article in Press, 2013.
13. Dubina, D., Ungureanu, V., *Effect of imperfections on numerical simulation of instability behaviour of cold-formed steel members*, Thin-Walled Structures, **40,** *3*, pp. 239–262, 2002.
14. Flores, F. G., Godoy, L. A., *Elastic postbuckling analysis via finite element and perturbation techniques*. *Part 1: Formulation*, Int. J. Numer. Meth. Eng., **33**, pp. 1775–1794, 1992.
15. Garcea, G., *Mixed formulation in Koiter analysis of thin-walled beam*, Comput. Methods Appl. Mech. Eng, **190**, pp. 3369–3399, 2001.
16. Garcea, G., Formica, G., Casciaro, R., *A numerical analysis of infinitesimal mechanisms*, Int. J. Numer. Meth. Eng., **62**, pp. 979–1012, 2005.
17. Garcea, G., Madeo, A., Casciaro, R., *The implicit corotational method and its use in the derivation of nonlinear structural models for beams and plates*, J. Mech. Mater. Struct, **7**, *6*, pp. 509–538, 2012.
18. Garcea, G., Madeo, A., Casciaro, R., *Nonlinear FEM analysis for beams and plate assemblages based on the Implicit Corotational Method*, J. Mech. Mater. Struct., **7**,*6*, pp. 539–574, 2012.
19. Garcea, G., Madeo, A., Zagari, G., Casciaro, R., *Asymptotic post-buckling FEM analysis using a corotational formulation*, Int. J. Solids Struct., **46**, *2*, pp. 523–532, 2009.
20. Garcea, G., Salerno, G., Casciaro, R., *Extrapolation locking and its sanitization in Koiter asymptotic analysis*, Comput. Methods Appl. Mech. Eng., **180**, *1–2*, pp. 137–167, 1999.
21. Garcea, G., Trunfio, G. A., Casciaro, R., *Mixed formulation and locking in path-following nonlinear analysis*, Comput. Methods Appl. Mech. Eng., **165**, *1–4*, pp. 247–272, 1998.
22. Garcea, G., G.A. Trunfio, Casciaro, R., *Path-following analysis of thin-walled structures and comparison with asymptotic post-critical solutions*, ComputInt. J. Numer. Meth. Eng., **55**, pp. 73–100, 2002.
23. Godoy, L. A., Banchio, E. G., *Singular perturbations for sensitivity analysis in symmetric bifurcation buckling*, Int. J. Numer. Meth. Eng., **52**, pp. 1465–1485, 2001.
24. Goltermann, P., Møllmann, H., *Interactive buckling in thin-walled beams – I. Theory*, Int. J. Solids Struct., **25**, pp. 715–749, 1989.
25. Ho, D., *The influence of imperfections on systems with coincident buckling loads*, Int. J. Non-Linear Mech., **7**, pp. 311–321, 1972.
26. Ho, D., *Buckling load of non-linear systems with multiple eigenvalues*, Int. J. Solids Struct., **10**, pp. 1315–1330, 1974.
27. Liang, K., Abdalla, M., G¨urdal, Z., *A Koiter-Newton approach for nonlinear structural analysis*, Int. J. Numer. Meth. Eng., **96**, *12*, pp. 763–786, 2013.
28. Koiter, W. T., *On the stability of elastic equilibrium*, Thesis, Delft, 1945. English transl. NASA TT-F10, 883, 1967 and AFFDL-TR70-25, 1970.

29. Koiter, W. T., *Some properties of (completely) symmetric multilinear forms with an application to Ho's theorem for multi-mode buckling*, Technologic University of Delft. Lab. Rep., 587, 1976.
30. Lanzo, A. D., Garcea, G., *Koiter analysis of thin-walled structures by a finite element approach*, Int. J. Numer. Meth. Eng., **39**, pp. 3007–3031, 1996.
31. Lanzo, A. D., Garcea, G., Casciaro, R., *Koiter post-buckling analysis of elastic plates*, Int. J. Numer. Meth. Eng., **38**, pp. 2325–2345, 1995.
32. Peek, R., Kheyrkhahan, M., *Postbuckling behavior and imperfection sensitivity of elastic structures by the Lyapunov-Schmidt-Koiter approach*, Comput. Methods Appl. Mech. Eng., **108**, *34*, pp. 261–279, 1993.
33. Poulsen, P.N., Damkilde, L., *Direct determination of asymptotic structural postbuckling behavior by the finite element method*, Int. J. Numer. Meth. Eng., **42**, *4*, pp. 685–702, 1998.
34. Salerno, G., Casciaro, R., *Mode jumping and attrative paths in multimode elastic buckling*, Int. J. Numer. Meth. Eng., **40**, pp. 833–861, 1997.
35. Schafer, B.W., Graham-Brady, L., *Sthocastic post-buckling of frames using Koiter's methods*, Int. J. Struct. Stab. Dyn., **6**, *3*, pp. 333–358, 2006.
36. Silvestre, N., Camotim, D., *Asymptotic-Numerical Method to Analyze the Postbuckling Behavior, imperfection-Sensitivity, and Mode Interaction in Frames*, Journal of Enginering Mechanics, **131**, *6*, pp. 617–632, 2005.
37. Sridharan, S., *Doubly symmetric interactive buckling of plate structures*, Journal J. Solids Struct., **19**, pp. 625–641, 1983.
38. Van Erp, G. M., Menken, C. M., *Initial post-buckling analysis with the spline finite-strip method*, Comput. Struct., **40**, pp. 1193–1201, 1991.
39. Wu, B., Wang, Z., *A perturbation method for the determination of the buckling strength of imperfection-sensitive structures*, Comput. Methods Appl. Mech. Eng., **145**, *3–4*, pp. 203–215, 1997.
40. Barbero, E.J. Madeo, A., Zagari, G., Zinno, R., Zucco, G., *Koiter asymptotic analysis of folded laminated composite plates*, Composites Part B: Eng., **61**, pp. 267–274, 2014.
41. Zagari, G., Madeo, A., Casciaro, R., de Miranda, S., Ubertini, F., *Koiter analysis of folded structures using a corotational approach*, Int. J. of Solids and Structures, **50**, *5*, pp. 755–765, 2013.